Optimal Range-Difference-Based Localization Considering Geometrical Constraints

Adrian N. Bishop, Barış Fidan, *Member, IEEE*, Brian D. O. Anderson, *Life Fellow, IEEE*, Kutluyıl Doğançay, *Senior Member, IEEE*, and Pubudu N. Pathirana, *Senior Member, IEEE*

***Abstract*—This paper proposes a new type of algorithm aimed at finding the traditional maximum-likelihood (TML) estimate of the position of a target given time-difference-of-arrival (TDOA) information, contaminated by noise. The novelty lies in the fact that a performance index, akin to but not identical with that in maximum likelihood (ML), is a minimized subject to a number of constraints, which flow from geometric constraints inherent in the underlying problem. The minimization is in a higher dimensional space than for TML, and has the advantage that the algorithm can be very straightforwardly and systematically initialized. Simulation evidence shows that failure to converge to a solution of the localization problem near the true value is less likely to occur with this new algorithm than with TML. This makes it attractive to use in adverse geometric situations.**

***Index Terms*—Localization, range difference, sensor networks, target tracking, time-difference-of-arrival (TDOA).**

I. Introduction

THE most common passive measurement technologies used today for localization and tracking are bearing measurements [1], [2] and time-difference-of-arrival (TDOA) or range-difference-of-arrival (RDOA) measurements. Received signal strength (RSS) is also used, permitting passive localization of an emitter whose power is known [3]. This paper focuses on TDOA-based (or RDOA-based) passive localization, with noise-contaminated measurements. TDOA or RDOA may be used to estimate the location of a wireless emitter or audio source, and there is considerable literature on the subject; see, for example, [4]–[9]. Underwater sonar has traditionally exploited TDOA methods for passive source localization [10] and motivates the work in this paper. The basic measurement parameter in TDOA is the TDOA of a signal (assumed to emanate isotropically from a source) as measured by pairs of spatially separated sensors (or receivers) at known locations. The resulting measurements give the range differences between the pairs of sensors with respect to the target and each such difference locates the target on a computable hyperbola in $\mathbb{R}^2$ or hyperboloid in $\mathbb{R}^3$, or actually, a branch of a hyperbola (or hyperboloid) when the sign of the range difference is taken into account. A sometimes desirable operational property exhibited by these techniques is that they inherently permit passive localization. That is, the sensors need only receive the signal from an emitter (e.g., audio, sonar, or radio source), and hence, the target need not be involved in or aware of the localization process. Indeed, in modern electronic warfare, it is particularly desirable to be able to locate a target without its knowledge [11], [12]. The intention of passive localization systems is to exploit the signals (e.g., radio or audio) generated by a target source (i.e., emitter) to locate the target without any active signal generation by the passive sensors.

TDOA-based localization has been a known technology since before World War II in one form or another [13] and is currently applicable in underwater sonar, electromagnetic radar, or acoustic-based systems. Much work has been focused on maximum-likelihood (ML) localization using TDOA [14]–[16] and a great deal of emphasis has also been placed on developing closed-form solutions [17]–[19], the determination of which typically involves a small number of calculations including operations such as matrix inversion. A number of these closed-form solutions introduce an artificial estimation error to account for the real measurement error [17], [18]. Other techniques [14], [16], [20] make assumptions on the probability density of the measurement errors and examine the problem from a purely statistical estimation point of view. None of these algorithms [14], [16]–[20] explicitly exploit the underlying geometrical properties of the required localization solution and the true measurement errors.

The objective of this work is to derive and examine functional relationships (which depend on the measurements and are rooted in geometry) between the measurement errors in a passive TDOA-based (or RDOA-based) localization scenario, and then to exploit them in a localization algorithm. The functional relationships are among the true values of certain quantities, but they are applied when noisy measurements arise. Broadly, we seek to form a constraint function that can be used in a constrained optimization process where the aim of the process is to minimize the location estimation error for a target. The constraint is a consequence of the underlying geometry. Indeed, the

Manuscript received December 16, 2007; revised April 16, 2008; accepted May 15, 2008. First published December 22, 2008; current version published January 16, 2009. The work of K. Doğançay was supported by the Defence Science and Technology Organisation (DSTO), Australia. The work of B. D. O. Anderson and B. Fidan was supported by the National ICT Australia. National ICT Australia is funded by the Australian Government's Department of Communications, Information Technology and the Arts and the Australian Research Council through the Backing Australia's Ability Initiative and the ICT Centre of Excellence Program. The work of P. N. Pathirana was supported by the Australian Research Council.

Associate Editor: D. A. Abraham.

A. N. Bishop is with the Royal Institute of Technology (KTH), Stockholm 10044, Sweden (e-mail: adrian.bishop@ieee.org).

B. Fidan and B. D. O. Anderson are with the National ICT Australia, Canberra, A.C.T. 2601, Australia and also with the Research School of Information Sciences and Engineering, Australian National University (ANU), Canberra, A.C.T. 0200, Australia (e-mail: baris.fidan@nicta.com.au; brian.anderson@anu.edu.au).

K. Doğançay is with the School of Electrical and Information Engineering, University of South Australia, Adelaide 5001, Australia (e-mail: kutluyil.dogancay@unisa.edu.au).

P. N. Pathirana is with Deakin University, Geelong 3217, Australia (e-mail: pubudu@deakin.edu.au).

Digital Object Identifier 10.1109/JOE.2008.926960

measurement errors may be estimated such that when measurements are corrected using estimates of these errors, and treated as if they were noiseless, it is straightforward to solve the resulting equations and guarantee that the solution is consistent with the underlying geometry, i.e., the geometric constraints are fulfilled.

Geometrical constraint-based optimization in localization systems is not new, and it may have been first introduced within the computer vision community [21]. In [21], the epipolar constraint is used to derive an optimal localization algorithm for stereo–vision systems. Geometric constraints have also been examined for distance-based and bearing-based localization problems in [22] and [23], respectively. Geometric constraints have also been exploited to improve localization using bearing and time-difference measurements in a multisensor hybrid localization system [24].

Using the geometric constraint we derive, we can then formulate the localization problem as a constrained optimization problem and compare our solution algorithm to a number of commonly employed techniques. In particular, we show that our algorithm with an appropriate choice of cost function and traditional maximum-likelihood (TML) algorithms, provided both algorithms converge, will deliver the same estimate. However, initialization to ensure convergence is more straightforward with the new algorithm, and as a consequence especially in adverse geometries, our algorithm outperforms TML. In addition, and not surprisingly, we show that our algorithm outperforms another class of algorithms, viewed as suboptimal in comparison with ML.

The remainder of this paper is organized as follows. In Section II, we discuss some related work in TDOA localization found in the literature. In Section III, we derive a functional relationship between the TDOA (or RDOA) measurement errors. In Section IV, we discuss how this error relationship may be used in a constrained optimization algorithm to optimally compute the location of the target. In Section V, we provide some numerical examples to compare our approach with the TML estimator and a closed-form linear approach to target localization. In Section VI, we outline some possible directions for future work, and in Section VII, we give our concluding remarks.

II. Prior Related Work

A. TML Algorithms

Under the usual Gaussian error assumptions, an ML algorithm for TDOA-based (or RDOA-based) localization requires a nonlinear least squares (LS) solver (e.g., Gauss–Newton) due to the nonlinearity of the problem [14], [16]. A search in 2-D or 3-D space is required to locate the minimum of a generally nonconvex function. (In contrast, our constrained optimization approach involves a search in a higher dimensional space than for ML, of a convex function, but subject to nonconvex constraints on the variables.) A modern opinion about TML and the initialization problem is as follows [9]: "selecting a good initial guess to avoid a local minimum is difficult and convergence is not guaranteed. An ML-based estimate is not suitable for real time implementation." Actually, despite the provably optimal characteristics of the ML estimate, the practical difficulties associated with finding the global optimal solution, i.e., of establishing a suitable algorithm to find the estimate, have long been a source of user hesitance in applying the TML approach.

B. Closed-Form Linear LS Algorithms

A number of papers [6], [17]–[19], [25] provide a closed-form LS solution to the TDOA-based (or RDOA-based) localization problem. By closed form, we mean that the computation does *not* involve iteration and obtains the position estimate through simple operations such as matrix inversion. We will not explore all of these techniques in this paper; suffice it to say that they all introduce an artificial estimation (or the so-called equation) error in place of accounting for the true measurement errors [18], [25], with the purpose of this change of view being to obtain a greatly simplified problem in a mathematical sense. Hence, none of the closed-form (LS) techniques can be considered to be ML estimators, despite the usual Gaussian assumptions and the use of apparent LS techniques (e.g., see [18] for a discussion on the "equation error" and the motivation of these closed-form pseudo-LS techniques). These closed-form techniques are known to be suboptimal [18] with the principal advantage of these techniques simply being the closed-form globally unique solution they provide. The primary disadvantage of these techniques is that in certain geometries and in high-noise scenarios, the final location estimate is likely to be highly erroneous due (in part) to a large estimation bias. In particular, as [9] notes, the spherical interpolation method of [18], established in [18] to be superior to several other closed-form methods, nevertheless fails to use certain redundant information and gives an error variance that may be large relative to the Cramér–Rao bound.

C. Constrained Weighted Linear LS Techniques

In [9] and [16], a slight variation to the linear LS cost function is made. A numerical algorithm is given that attempts to find a global extremum of the new cost function, and thus a unique location solution. This novel variation is based around enforcing a single constraint between the simultaneously estimated target position and target range and attempts to ensure that a globally minimum solution can be found even when numerical solvers are employed. As with TML, this algorithm also requires an initial estimate of the target location [16] and convergence to the correct solution may or may not occur, depending on the quality of this estimate. Note that this technique, when it converges, does not give a location solution, which is provably equivalent to the ML estimate, i.e., this approach is not optimal in the ML sense.

III. A Geometric Constraint on the Measurement Errors

The prime purpose of this section is to describe how equations can be derived that incorporate noisy measurements, and that serve to constrain the errors associated with those measurements, by virtue of the underlying geometry. The measurements acquired in TDOA systems are the arrival times at each sensor of an emitter signal, and the inferring by subtraction of range differences to the emitter. Let $i \in \{1, \ldots, n\}$ index the sensors and without loss of generality we place sensor 1 at the origin.

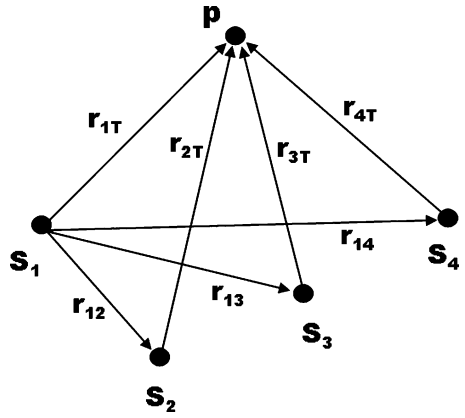

Fig. 1. Example of a TDOA scenario with four sensors located at the points $\mathbf{s}_i$ and a single target located at $\mathbf{p}$.

Let the column vector between sensors 1 and $i \neq 1$ be denoted by $\mathbf{r}_{1i}$ and assume these vectors are known for all i. Finally, let the column vector between sensor i and the target be denoted by $\mathbf{r}_{iT}$. The scenario for $\mathbb{R}^2$ is depicted in Fig. 1 with four sensors.

In this paper, we consider the general problem involving $q+2$ or more sensors in q dimensions where $q = 2$ or $q = 3$. Each sensor $i \in \{1, \ldots, n\}$ measures the time of signal arrival

$$\widehat{t}_i = \frac{\|\mathbf{r}_{iT}\|}{v} + \epsilon_i \tag{1}$$

where v is the signal propagation speed and ϵ_i is the timing error. A system of $n \geq q+2$ sensors then provides $n-1$ TDOA measurements that in the noiseless case are described by $t_i - t_1$ for $i \in \{2, \ldots, n\}$. The noisy TDOA measurements are given by

$$\widehat{t}_{1i} = \frac{\|\mathbf{r}_{iT}\|}{v} + \epsilon_i - \frac{\|\mathbf{r}_{1T}\|}{v} - \epsilon_1. \tag{2}$$

Multiplying each true time-difference $t_i - t_1$ by v gives a system of true range-difference measurements

$$d_{1i} = \|\mathbf{r}_{iT}\| - \|\mathbf{r}_{1T}\| = v(t_i - t_1) \tag{3}$$

while, similarly, multiplying the noisy TDOA measurement $\widehat{t}_{1i} = \widehat{t}_i - \widehat{t}_1$ by v leads to a system of noise corrupted range-difference measurements

$$\widehat{d}_{1i} = \|\mathbf{r}_{iT}\| - \|\mathbf{r}_{1T}\| + v(\epsilon_i - \epsilon_1) = d_{1i} + e_{1i} \tag{4}$$

where $e_{1i} = v(\epsilon_i - \epsilon_1)$ is the so-called range-difference measurement error. Note that throughout this paper it is assumed that the value of v is a constant and is known accurately. Moreover, in this paper, we work directly with the range-difference measurement equations (4) when discussing the localization algorithm.

At this stage, it is necessary to postulate statistical properties for the noise in (4), which reflect its physical origins. Following [8], we will assume that the prime source of the range-difference errors e_{1i} is the presence of individual timing errors ϵ_i in each receiver. We postulate that these timing errors are zero mean, Gaussian, and independent, with the same variance σ_t^2. Then, the range-difference measurement errors e_{1i}, $\forall\{2, \ldots, n\}$, are correlated and have covariance matrix Σ given by

$$\mathbf{\Sigma} = \sigma_d^2 \begin{bmatrix} 1 & \frac{1}{2} & \cdots & \frac{1}{2} \\ \frac{1}{2} & \ddots & \ddots & \vdots \\ \vdots & \ddots & \ddots & \frac{1}{2} \\ \frac{1}{2} & \cdots & \frac{1}{2} & 1 \end{bmatrix} \tag{5}$$

where $\sigma_d^2 = 2v^2\sigma_t^2$ is the variance of an individual range-difference measurement.[1] Note that the mean of e_{1i}, $\forall\{2, \ldots, n\}$, remains zero.

The $n-1$ measurements (4) define $n-1$ hyperbolas (or hyperboloids) in q-dimensional space whose foci points correspond to the two sensor locations used in defining the hyperbola (3). More specifically, the sign of the measurements determines on which branch of the hyperbola the target lies. In generic geometries, $n = q+2$ sensors are necessary and sufficient to uniquely localize a target in $\mathbb{R}^q$. Note that $q+2$ sensors give rise to $q+1$ independent TDOA measurements, and thus the equations for the target position in the noiseless case will be overdetermined. The problem with using only q independent TDOA measurements is that the defining equations have multiple solutions in q dimensions, e.g., two (coplanar) hyperbolas, in general, will intersect in more than one point. On the other hand, once noise is present, the overdetermined equations will have no solution, and that is why the noisy localization problem is nontrivial. Let us note as well the importance of the word "generic." If all sensors are collinear and the target is in between any two sensors and collinear with them, which is a nongeneric configuration, then no matter how many sensors there are, one has an ambiguity even in the noiseless case in localizing the target.

The following result captures the constraints among the e_{1i} that are expressible using the noisy measurements, and it flows from the underlying geometry.

Theorem 1: In $\mathbb{R}^q$ ($q \in \{2, 3\}$), assume $n = q+2$ sensors define $n-1$ range-difference measurements based on the models (3) and (4); then, a constraint equation on the measurement errors can be given in terms of the known sensor coordinates and the noisy measurements as

$$\operatorname{diag}(\overline{\mathbf{P}})^{\mathrm{T}} \overline{\mathbf{P}}^{-1} \operatorname{diag}(\overline{\mathbf{P}}) = 0 \tag{6}$$

where $\operatorname{diag}(\overline{\mathbf{P}})$ is the vector of diagonal elements of the $(q+1) \times (q+1)$ matrix $\overline{\mathbf{P}} = \overline{\mathbf{A}} \Lambda \overline{\mathbf{A}}^{\mathrm{T}}$, the $(q+1) \times (q+1)$ matrix $\overline{\mathbf{A}}$ is given by

$$\overline{\mathbf{A}} = \begin{bmatrix} \mathbf{r}_{12}^{\mathrm{T}} & \widehat{d}_{12} - e_{12} \\ \mathbf{r}_{13}^{\mathrm{T}} & \widehat{d}_{13} - e_{13} \\ \vdots & \vdots \\ \mathbf{r}_{1n}^{\mathrm{T}} & \widehat{d}_{1n} - e_{1n} \end{bmatrix} \tag{7}$$

and $\Lambda = \operatorname{diag}(1\ 1 - 1)$ or $\Lambda = \operatorname{diag}(1\ 1\ 1 - 1)$ when $q = 2$ or $q = 3$, respectively.

Proof: Applying the law of cosines to the system of $q+1$ triangles defined by the target, sensor 1, and sensor i, $\forall i \in \{2, \ldots, q+2\}$, gives $q+1$ equations of the form

$$\|\mathbf{r}_{iT}\|^2 = \|\mathbf{r}_{1T}\|^2 + \|\mathbf{r}_{1i}\|^2 - 2\mathbf{r}_{1i}^{\mathrm{T}}\mathbf{r}_{1T}. \tag{8}$$

[1]It would appear that the closed-form techniques may implicitly assume a different noise model in which independent errors are postulated in the individual TDOA measurements, though it is hard to understand the physical basis for this.

Now if we square (3), we obtain

$$\|\mathbf{r}_{iT}\|^2 = d_{1i}^2 + \|\mathbf{r}_{1T}\|^2 + 2d_{1i}\|\mathbf{r}_{1T}\| \tag{9}$$

and then substituting this into (8), we obtain $n-1$ equations of the form

$$2\left[\mathbf{r}_{1i}^{\mathrm{T}}\ d_{1i}\right]\begin{bmatrix}\mathbf{r}_{1T}\\ \|\mathbf{r}_{1T}\|\end{bmatrix} = \left(\|\mathbf{r}_{1i}\|^2 - d_{1i}^2\right). \tag{10}$$

We can stack the resulting $n-1$ equations to give

$$2\mathbf{A}\begin{bmatrix}\mathbf{r}_{1T}\\ \|\mathbf{r}_{1T}\|\end{bmatrix} = \mathbf{b} \tag{11}$$

where

$$\mathbf{A} = \begin{bmatrix}\mathbf{r}_{12}^{\mathrm{T}} & d_{12}\\ \mathbf{r}_{13}^{\mathrm{T}} & d_{13}\\ \vdots & \vdots\\ \mathbf{r}_{1n}^{\mathrm{T}} & d_{1n}\end{bmatrix}, \quad \mathbf{b} = \begin{bmatrix}\|\mathbf{r}_{12}\|^2 - d_{12}^2\\ \|\mathbf{r}_{13}\|^2 - d_{13}^2\\ \vdots\\ \|\mathbf{r}_{1n}\|^2 - d_{1n}^2\end{bmatrix}. \tag{12}$$

Therefore, assuming $\mathbf{A}$ is nonsingular,[2] we obtain

$$\begin{bmatrix}\mathbf{r}_{1T}\\ \|\mathbf{r}_{1T}\|\end{bmatrix} = (2\mathbf{A})^{-1}\mathbf{b}. \tag{13}$$

Letting $(2\mathbf{A})^{-1}\mathbf{b} = [\beta_1\ \beta_2\ \cdots\ \beta_{(n-1)}]^{\mathrm{T}}$, it is straightforward to conclude that

$$\beta_1^2 + \beta_2^2 + \cdots + \beta_{(n-2)}^2 - \beta_{(n-1)}^2 = 0. \tag{14}$$

The expression (14) can be simplified by defining $\mathbf{P} = \mathbf{A}\Lambda\mathbf{A}^T$ and noting that

$$\mathrm{diag}(\mathbf{P})^{\mathrm{T}}\mathbf{P}^{-1}\mathrm{diag}(\mathbf{P}) = 0 \tag{15}$$

where $\mathrm{diag}(\mathbf{P}) = \mathbf{b}$ is the column vector of the diagonal elements of $\mathbf{P}$. Now the constraint (6) follows directly from the constraint (15) with $d_{1i} = \widehat{d}_{1i} - e_{1i}$ and such that $\overline{\mathbf{A}} = \mathbf{A}$ with $d_{1i} = \widehat{d}_{1i} - e_{1i}$. Thus, we have a constraint (6) on the unknown measurement errors e_{1i} with known parameters given by the sensor coordinates and the noisy measured values $\widehat{d}_{1i}$. ■

To justify the development of Theorem 1, we offer the following remark.

Remark 1: Suppose that noise is present in the measurements. If we acted as if the measurements were noiseless and obtained and plotted the hyperbolic branches of interest, we would find that there would not be, in general, a single point of intersection of all the branches. We are providing a tool to address this problem by first identifying a constraint (Theorem 1) on the measurement errors reflecting the fact that if the errors giving rise to the noisy hyperbolic branches respected the constraint then there would happen to be a unique point of intersection after correcting the errors. Therefore, once we have noisy measurements, we find (via Theorem 1) that the e_{1i} cannot assume arbitrary values because that would be inconsistent with the hyperbola branches having a unique point of intersection.

Remark 2: The calculations in Theorem 1 are very similar to those used in the closed-form solution approach. The closed-form solution to range-difference-based localization is based on the construction of a matrix $\widehat{\mathbf{A}}$ whose first q columns are identical to those of $\overline{\mathbf{A}}$ and whose last column includes the noisy measurements $\widehat{d}_{1i}$. One also constructs a vector $\widehat{\mathbf{b}}$ based on the noisy values $\widehat{d}_{1i}$. That is, the matrix $\widehat{\mathbf{A}}$ and the vector $\widehat{\mathbf{b}}$ are given by

$$\widehat{\mathbf{A}} = \begin{bmatrix}\mathbf{r}_{12}^{\mathrm{T}} & \widehat{d}_{12}\\ \mathbf{r}_{13}^{\mathrm{T}} & \widehat{d}_{13}\\ \vdots & \vdots\\ \mathbf{r}_{1n}^{\mathrm{T}} & \widehat{d}_{1n}\end{bmatrix}, \quad \widehat{\mathbf{b}} = \begin{bmatrix}\|\mathbf{r}_{12}\|^2 - \widehat{d}_{12}^2\\ \|\mathbf{r}_{13}\|^2 - \widehat{d}_{13}^2\\ \vdots\\ \|\mathbf{r}_{1n}\|^2 - \widehat{d}_{1n}^2\end{bmatrix} \tag{16}$$

and the closed-form target estimate is found by solving $(2\widehat{\mathbf{A}})^{-1}\widehat{\mathbf{b}}$. Contrast this expression with (13) where in $\mathbf{A}$ and $\mathbf{b}$ the value of each range-difference is the true value, despite the ability to express this value using noisy measurements and error values, i.e., $d_{1i} = \widehat{d}_{1i} - e_{1i}$. Now because on the right-hand side of (13) true values appear (albeit expressible using noisy measurements and noise values), the vector on the left-hand side necessarily has the property that the Euclidean norm of its first q entries is equal to the last entry. This leads to the given constraint (6) on the measurement errors with known parameters given by the sensor coordinates and the noisy measured values. However, this constraint property will not generally hold for $(2\widehat{\mathbf{A}})^{-1}\widehat{\mathbf{b}}$ because the noisy measured values are used, essentially with the assumption that $e_{1i} = 0, \forall i \neq 1$. However, by throwing away the information in the last entry of $(2\widehat{\mathbf{A}})^{-1}\widehat{\mathbf{b}}$, the first q entries can be used to provide an estimate (albeit one that may have substantial bias depending on the particular localization geometry), or alternatively, an initial iterate for a numerical iterative algorithm, such as TML. The bias effect can be reduced by increasing the number of sensors or using sensors that yield a lower measurement noise variance. This approach, which is essentially the "spherical interpolation" method of [18] is analyzed and improved upon somewhat in [9].

A. Increasing the Number of Sensors and Independent Geometric Constraints

We can derive a system of functional relationships on the measurement errors for the scenarios involving more than $q+2$ sensors in $\mathbb{R}^q$. If the system involves $n \geq q+2$ sensors, then we have $n-(q+1)$ independent constraints (the notion of independent constraint is probably intuitively clear, but it is explained in more detail below) and we can write them in the form

$$c_{i-(q+1)}\left(e_{12}, e_{13}, \ldots, e_{1q}, e_{1(q+1)}, e_{1i}\right) = 0 \tag{17}$$

for all $i \in \{q+2, \ldots, n\}$. These equations are obtained by considering the measurement and geometrical relations (as previously shown) between the sensors $\{1, 2, \ldots, q+1\}$ and i, for $i \in \{q+2, \ldots, n\}$. Therefore, let the column vector of constraint functions be denoted by

$$\mathbf{c}(\mathbf{e}) = \begin{bmatrix}c_1\left(e_{12}, e_{13}, \ldots, e_{1q+1}, e_{1(q+2)}\right)\\ \vdots\\ c_{n-(q+1)}\left(e_{12}, e_{13}, \ldots, e_{1(q+1)}, e_{1n}\right)\end{bmatrix} \tag{18}$$

where $\mathbf{e}$ is the vector of measurement errors. Now let us explain the notion of independent and dependent constraints. The first two entries in (18) arise from considering relations between the sensor sets $\{1, 2, \ldots, q+1, q+2\}$ and

[2]For generic, and thus almost all values of sensor positions, $\mathbf{A}$ will be nonsingular. However, there will be special values where this is not the case, corresponding to nongeneric situations, for example, when all sensors are collinear with the target. More generally, "bad geometries" will be those where $\mathbf{A}$ is ill conditioned.

$\{1, 2, \ldots, q+1, q+3\}$. We could also obtain a relation among the sensors in the set $\{1, 2, \ldots, q, q+2, q+3\}$, which would be $\bar{c}(e_{12}, e_{13}, \ldots, e_{1q}, e_{1(q+2)}, e_{1(q+3)}) = 0$. This would not be independent of the first two entries in (18) because it could be derived from them. In other words, if we did write down this constraint, it would not give us any more information about the e_i that we did not already have. At a very simple level, what we are saying is that if one has a TDOA involving sensors 1 and 2, and a second TDOA involving sensors 2 and 3, it is trivial to obtain the TDOA involving sensors 1 and 3, whether timing errors are present. The question of which pair of the three TDOAs it is better to use is almost a nonquestion. We note that any set of independent constraints could be chosen and that the particular choice should not influence the way the iterative algorithm of Section IV behaves, apart from changing the conditioning of calculations that might be required at each step of the algorithm.

IV. The Constrained Optimization Approach

The constraints on the measurement errors discussed in Section III can be used in finding an optimal solution to the localization problem after formulating the localization problem as a constrained optimization problem [26], [27]. In this paper, we will illustrate the proposed concept via a constrained LS optimization problem. Assuming zero-mean Gaussian errors, we consider the following objective function:

$$f(\mathbf{e}) = \mathbf{e}^{\mathrm{T}} \boldsymbol{\Sigma}^{-1} \mathbf{e} \tag{19}$$

where $\mathbf{e}$ is a column vector of the errors $e_{12}, e_{13}, e_{14}, \ldots, e_{1n}$ and $\boldsymbol{\Sigma}$ is the error covariance matrix [typically given by (5)]. We want to minimize the cost function (19) subject to the system of constraints $c_{i-q}(e_{12}, e_{13}, \ldots, e_{1(q+1)}, e_{1i}) = 0$ for $i \in \{q+2, \ldots, n\}$ in $\mathbb{R}^q$. Given the postulate of a Gaussian *a priori* density for the measurement errors, we are actually maximizing the *a posteriori* density when we minimize (19) subject to the system of constraints; the system of constraints of course reflects the measurements.

Note that the cost function (19) is on the actual errors and would achieve a minimum value of zero if we did not subject the minimization to the satisfaction of the constraints. Minimizing the LS cost function (19) subject to the constraints is in principle equivalent to minimizing the (nonlinear LS) TML cost function given in [14] and [16]. Despite the theoretical similarities between the two approaches, the practical techniques used to actually compute the ML target estimate will obviously differ for the two approaches. The dimensions of the underlying space in which the iterations are carried out are clearly different and the initializations are different. Accordingly, it is not surprising that a key performance measure, viz., the ability to converge to a solution near the true value, is different. While no absolute guarantee of such convergence can be given in relation to the algorithm we will propose, simulations and heuristic reasoning suggest that in "adverse" geometries, it will perform much better than TML, while in nonadverse geometries, there is no essential difference. In fact, in nonadverse localization geometries, the linear LS methods, e.g., see Remark 2, are likely to compare favorably with the ML algorithms and are much easier to implement.

A. Optimization Algorithm Reflecting the Geometrically Induced Nonlinear Constraints

Due to the nonlinearity of the constraints, we employ the widely used sequential quadratic programming (SQP) technique [26], [28] to perform the optimization associated with (19). SQP mimics Newton's method for unconstrained optimization. Consider the following objective function $f(\mathbf{e})$ on the relevant measurement errors. The function $f(\mathbf{e})$ captures the desired metric of the measurement errors to be minimized, e.g., the squared ℓ_2-norm. Consider the following general nonlinear programming problem:

$$\begin{aligned} \arg\min_{\mathbf{e}} \quad & f(\mathbf{e}) \\ \text{s.t.} \quad & \mathbf{c}(\mathbf{e}) = \mathbf{0} \end{aligned} \tag{20}$$

where $f(\mathbf{e})$ is a given cost function and $\mathbf{c}(\mathbf{e})$ is the column vector of constraint functions. In general, the vector of constraint functions $\mathbf{c}(\mathbf{e})$ is nonlinear and nonconvex. Thus, the nonlinear programming methods, which rely on iteration and initial estimates, are likely to be required. In this chapter, a method of numerical solution is given to the general nonlinear programming problem (20). SQP [26], [28] mimics Newton's method for unconstrained optimization and is used to solve the problem (20).

Assume both the Jacobian and the Hessian exist for the objective and the constraint in (20). The Lagrangian function associated with the problem (20) is given by

$$\mathcal{L} = f(\mathbf{e}) + \boldsymbol{\lambda}^{\mathrm{T}} \mathbf{c}(\mathbf{e}) \tag{21}$$

where $\boldsymbol{\lambda}$ is a column vector of Lagrange multipliers. A minimum of the Lagrangian (21) occurs when

$$\nabla \mathcal{L} = \begin{bmatrix} \nabla_{\mathbf{e}} f(\mathbf{e})^{\mathrm{T}} + \nabla_{\mathbf{e}} \mathbf{c}(\mathbf{e})^{\mathrm{T}} \boldsymbol{\lambda} \\ \mathbf{c}(\mathbf{e}) \end{bmatrix} = \begin{bmatrix} 0 \\ 0 \end{bmatrix} \tag{22}$$

for some $\boldsymbol{\lambda}$ and for some $\mathbf{e}$. It is possible to define an iterative procedure for finding an optimal error solution and an optimal Lagrange multiplier vector satisfying (22). The iterations must begin with an estimate $\mathbf{e}_0$ and $\boldsymbol{\lambda}_0$. Then, the iteratively updated estimates of $\mathbf{e}$ and $\boldsymbol{\lambda}$ are calculated by

$$\mathbf{e}_{k+1} = \mathbf{e}_k + \alpha_k \mathbf{q}_k \tag{23}$$

$$\boldsymbol{\lambda}_{k+1} = \boldsymbol{\lambda}_k + \alpha_k \boldsymbol{\nu}_k \tag{24}$$

where α_k is an adjustable step-size parameter (to be discussed subsequently). Here, $\mathbf{q}_k$ and $\boldsymbol{\nu}_k$ are the increments that should drive $\mathbf{e}_k$ and $\boldsymbol{\lambda}_k$ toward a solution of (22). The increments can be obtained by solving a quadratic optimization (sub)problem that is designed to approximate (20) given an estimate $\mathbf{e}_k$ and $\boldsymbol{\lambda}_k$ [29].

At the kth iteration, let $\mathbf{e}_k$ be an estimate of the optimal error solution and let $\boldsymbol{\lambda}_k$ be an estimate of the associated optimal Lagrange multiplier vector. Then, it is possible to approximate the problem (20) by the following quadratic programming problem:

$$\begin{aligned} \arg\min_{\mathbf{q}} \quad & \frac{1}{2} \mathbf{q}_k^{\mathrm{T}} \mathcal{H}\left(\mathcal{L}(\mathbf{e}_k, \boldsymbol{\lambda}_k)\right) \mathbf{q}_k + \mathcal{J}\left(f(\mathbf{e}_k)\right) \mathbf{q}_k \\ \text{s.t.} \quad & \mathcal{J}\left(\mathbf{c}(\mathbf{e}_k)\right) \mathbf{q}_k + \mathbf{c}(\mathbf{e}_k) = 0 \end{aligned} \tag{25}$$

where $\mathcal{J}(f(\mathbf{e}_k))$ is the Jacobian of the cost function evaluated at $\mathbf{e} = \mathbf{e}_k$ and $\mathcal{H}(\mathcal{L}(\mathbf{e}_k, \boldsymbol{\lambda}_k))$ is the Hessian of the Lagrangian (21) with respect to $\mathbf{e}$ and evaluated at $\mathbf{e} = \mathbf{e}_k$ and $\boldsymbol{\lambda} = \boldsymbol{\lambda}_k$. Moreover, $\mathcal{J}(\mathbf{c}(\mathbf{e}_k))$ is the Jacobian of the constraint vector and $\mathbf{c}(\mathbf{e}_k)$ is the column vector of the constraint functions evaluated at $\mathbf{e}_k$. Now consider the Lagrangian of the quadratic approximation (25) that is given by

$$\widetilde{\mathcal{L}} = \left(\frac{1}{2}\mathbf{q}_k^{\mathrm{T}}\mathcal{H}\left(\mathcal{L}(\mathbf{e}_k, \boldsymbol{\lambda}_k)\right)\mathbf{q}_k + \mathcal{J}\left(f(\mathbf{e}_k)\right)\mathbf{q}_k\right) + \boldsymbol{\nu}_k^{\mathrm{T}}\left(\mathcal{J}\left(\mathbf{c}(\mathbf{e}_k)\right)\mathbf{q}_k + \mathbf{c}(\mathbf{e}_k)\right) \quad (26)$$

where $\boldsymbol{\nu}_k$ is the relevant vector of Lagrange multipliers. Replicating (22) for the Lagrangian (26) leads to the following first-order necessary conditions for a minimum:

$$\nabla\widetilde{\mathcal{L}} = \begin{bmatrix} \mathcal{H}\left(\mathcal{L}(\mathbf{e}_k, \boldsymbol{\lambda}_k)\right)\mathbf{q}_k + \mathcal{J}\left(f(\mathbf{e}_k)\right)^{\mathrm{T}} + \mathcal{J}\left(\mathbf{c}(\mathbf{e}_k)\right)^{\mathrm{T}}\boldsymbol{\nu}_k \\ \mathcal{J}\left(\mathbf{c}(\mathbf{e}_k)\right)\mathbf{q}_k + \mathbf{c}(\mathbf{e}_k) \end{bmatrix} = \begin{bmatrix} 0 \\ 0 \end{bmatrix}. \quad (27)$$

Thus, a solution $\mathbf{q}_k$ and $\boldsymbol{\nu}_k$ solves the problem (25) if and only if the standard Karush–Kuhn–Tucker (KKT) equations [27] are satisfied with some $\boldsymbol{\nu}_k$ and $\mathbf{q}_k$. That is, if

$$\mathbf{G}\begin{bmatrix} \mathbf{q}_k \\ \boldsymbol{\nu}_k \end{bmatrix} = -\begin{bmatrix} \mathcal{J}\left(f(\mathbf{e}_k)\right)^{\mathrm{T}} \\ \mathbf{c}(\mathbf{e}_k) \end{bmatrix} \quad (28)$$

where

$$\mathbf{G} = \begin{bmatrix} \mathcal{H}\left(\mathcal{L}(\mathbf{e}_k, \boldsymbol{\lambda}_k)\right) & \mathcal{J}\left(\mathbf{c}(\mathbf{e}_k)\right)^{\mathrm{T}} \\ \mathcal{J}\left(\mathbf{c}(\mathbf{e}_k)\right) & 0 \end{bmatrix} \quad (29)$$

are satisfied for some $\mathbf{q}_k$ and $\boldsymbol{\nu}_k$. Note that a solution to the linear system (28) will always exist when the Hessian and the Jacobian of the constraint vector are nonsingular.

The SQP technique seeks to solve the equations provided by the first-order (necessary) optimality conditions using a Newton iteration (or Lagrange–Newton iteration). The algorithm is iterative and terminates when the step change is less than a predetermined tolerance $\gamma \geq 0$ such that $\|\mathbf{e}_{k+1} - \mathbf{e}_k\| \leq \gamma$ at which point the optimal error estimate is given by $\mathbf{e}_{k+1}$.

The line-search step-size parameter α_k should be chosen such that $f(\mathbf{e}_k + \alpha_k\mathbf{q}_k)$ is minimized, i.e., α_k should be selected to ensure $\mathbf{e}_{k+1}$ is an improved solution. However, it is often more computationally convenient to find α_k such that there is a *sufficient* decrease in $f(\mathbf{e}_k + \alpha_k\mathbf{q}_k)$ as opposed to finding the explicit minimum (which is particularly hazardous if $f(\cdot)$ is nonconvex). One possible method of choosing the step parameter α_k is to find one that satisfies the Wolfe conditions [30], [31] given by

$$f(\mathbf{e}_k + \alpha_k\mathbf{q}_k) \leq f(\mathbf{e}_k) + c_1\alpha_k\mathcal{J}\left(f(\mathbf{e}_k)\right)\mathbf{q}_k \quad (30)$$

$$\left|\mathcal{J}\left(f(\mathbf{e}_k + \alpha_k\mathbf{q}_k)\right)\mathbf{q}_k\right| \leq c_2\left|\mathcal{J}\left(f(\mathbf{e}_k)\right)\mathbf{q}_k\right| \quad (31)$$

for some $0 < c_1, c_2 < 1$. The first condition ensures a *sufficient* decrease is achieved with a given step parameter $\alpha_k \in \mathbb{R}$, while the second condition ensures that α_k does indeed lie close to a (local) minimizer of $f(\mathbf{e}_k + \alpha_k\mathbf{q}_k)$.

Note that the implementation of SQP considered thus far requires the Hessian to exist and be nonsingular at $\mathbf{e}_k$. If this requirement holds and the Hessian is positive definite in a neighborhood enclosing a critical point and $\mathbf{e}_0$ is chosen to lie within this neighborhood, then the algorithm converges at a quadratic rate.

A logical choice for the initial error estimate is $\mathbf{e}_0 = \mathbf{0}$ (assuming zero-mean errors). Considering that the majority of optimization algorithms for localization require an initial estimate of the unknown target location, our formulation offers a simple yet particularly important (problem-invariant) advantage over traditional optimization algorithms. In fact, it is well known that the initial estimate plays a crucial role in the convergence and performance of many traditional optimization algorithms for localization.

B. Following the Optimization

Following the convergence of the optimization algorithm, we have an estimate of the errors. According to the constraints on the measurement errors given in the previous sections and (4), it is this error value *subtracted* from the corresponding *measured* range-difference value that results in system consistency along with correction of the data allowing estimation of the true range-difference values. That is, according to (4), if the estimated errors were equal to the true error values, then subtracting these values to the actual measured values of the range differences would result in us knowing the true (and thus geometrically consistent) range differences. Of course, we can only hope to determine an optimal (and geometrically consistent) estimate of the actual measurement error values and hence an optimal estimate of the true range differences.

Once we have estimated the measurement errors and performed the measurement *correction* as it may be called, it should be possible to solve the overdetermined systems of measurement equations for a geometrically consistent (and optimal in the sense of constrained minimum errors) target location estimate. Closed-form solutions to the general nonlinear TDOA measurement equations are simple to derive and are applicable, e.g., see Remark 2.

C. Estimation Error Covariance

The target position estimate that our approach ultimately seeks to find is equivalent to that which the TML approach seeks to find. Essentially, both approaches rely on different parameterizations of the more general ML estimation problem. The practical techniques used to find that position estimate (i.e., the ML estimate) obviously differ for the two approaches. However, it follows that the bias and variance calculations on the position estimate for TML apply equally to our algorithm at the global minimum (i.e., when our algorithm has converged appropriately). Indeed, it is known [32] that, asymptotically, the variance of an ML estimate approaches the Cramér–Rao bound. Therefore, as the number of measurements increases, the bias of the constrained LS optimization algorithm approaches zero and the variance approaches the Cramér–Rao lower bound. For a finite number of measurements, the specific estimator bias and variance can be determined similarly to [2] for bearing-only

ML localization. See also [33] for a discussion on the error variance of TDOA-based ML localization.

D. Algorithm Assumptions and Robustness Tradeoffs

The algorithm development has so far assumed that the measurement errors were Gaussian in nature. Thus, an LS cost function was utilized to achieve an ML estimation algorithm. The error statistics were assumed to be known accurately and, in particular, the structure of the covariance matrix was required to achieve a true ML estimate. In this section, we discuss the potential of modifying the optimization/estimation algorithm developed in this paper to account for unknown or partially known error statistics or different error distributions.

First, note that as long as the measurement errors are Gaussian and the covariance matrix can be accurately derived using known error statistics, then a true ML estimation algorithm can be formulated as illustrated in this section. Of course, implicit in this statement is the assumption that the error statistics are independent of the true target position.

If the errors are known to be Gaussian but the exact statistics and correlations are not known accurately, then the LS-based algorithm developed in this section can provide a good approximation to the true ML estimator. The identity matrix is potentially the most robust choice for the covariance matrix in the absence of any additional information.

More generally, note that the estimation algorithm developed in this section is adaptable to other cost functions, i.e., other than LS cost functions such as (19). The LS approach is equivalent to the ML approach under Gaussian error assumptions. However, there may be cases when a different cost function (e.g., some ℓ_p-norm with $p \neq 2$) is better suited to the problem [34]. For example, the ℓ_1-norm is generally considered more robust against large outliers. Note that the geometric constraint is independent of the specific measurement error distribution or statistics. Thus, any chosen cost function can be substituted in place of (19), e.g., when the errors are not Gaussian. In the case of unknown measurement error distributions, the proposed algorithm makes it feasible to experiment (during system calibration) with different cost functions. Essentially, the tradeoff between algorithm robustness and optimality can be tuned by adjusting the cost function.

V. Numerical Examples

To illustrate our geometrically constrained optimization approach to TDOA-based localization in $\mathbb{R}^2$, we will now explore three localization examples. We compare the quality of the localization solutions obtained from our geometrically constrained optimization approach incorporating a weighted LS cost function (19) (denoted GCLS) against the quality of those obtained via TML implemented using a Gauss–Newton algorithm [14], [16], [20] (denoted TML-GN). We also compare directly with the closed-form solution discussed in Remark 2 and the Cramér–Rao bound; see, e.g., [8] and [18]. The GCLS method is initialized with $\mathbf{e} = \mathbf{0}$ while the TML-GN method (as is common, though perhaps not universal) is initialized with the closed-form pseudo-LS estimate discussed in Remark 2. Both numerical algorithms (i.e., GCLS and TML-GN) are terminated when the size of the step change is below a given tolerance value or when the number of iterations exceeds a given maximum threshold.

Remark 3: Although the stopping criteria for GCLS and TML-GN are of the same form, the iterated estimates (which are not even vectors of the same dimension) and hence the step changes in the algorithm are not of the same nature. In the TML-GN algorithm, the length of the step change can be given by $\delta_{\mathbf{p}k} = \|\mathbf{p}_{k+1} - \mathbf{p}_k\|$ where $\mathbf{p}_k$ is the position estimate at the kth iteration of the Gauss–Newton-based TML-GN algorithm [16]. In the GCLS algorithm, the length of the step change is given by $\delta_{\mathbf{e}k} = \|\mathbf{e}_{k+1} - \mathbf{e}_k\|$, which is the change in the estimate of the range-difference (TDOA) measurement error vector. However, for a certain fictitious position estimate $\widetilde{\mathbf{p}}_k$ defined at each step by employing the iterated estimate $\mathbf{e}_k$, it so happens that $\delta_{\mathbf{e}k}$ can be related to $\delta_{\widetilde{\mathbf{p}}k} = \|\widetilde{\mathbf{p}}_{k+1} - \widetilde{\mathbf{p}}_k\|$, which is of the same nature as $\delta_{\mathbf{p}k}$. Details of the fictitious position estimate $\widetilde{\mathbf{p}}_k$ and the corresponding relationship between $\delta_{\mathbf{e}k}$ and $\delta_{\widetilde{\mathbf{p}}k}$ are given in the Appendix.

Thus, it is this observation that justifies the use of the same stopping criteria for both numerical algorithms.

Remark 4: In the examples below, we contrast problems with good and bad geometry. While these terms have intuitive meaning, it should be noted that the concept of geometry quality can be given quantitative content; e.g., see [35]–[38]. Informally, we note that when the average target range-to-sensor-baseline ratio is large, then the target appears almost collinear with the sensors. In this case, the *localization geometry* is adversely suited to accurate localization. See also [36]–[38] for an explicit characterization of localization geometries using the Fisher information matrix along with [35] for a discussion on localization sensitivity and conditioning.

The individual timing measurement errors are assumed to be independent Gaussian random variables with a variance given by σ_t^2. Therefore, the time-difference (or range-difference) measurement errors are correlated and the covariance matrix of the range-difference measurement vector $\mathbf{\Sigma}$ is given by (5). The values chosen to represent the error statistics σ_d^2 in simulation are consistent with the literature; e.g., see [8] and [16].

A. Simulation Case 1

The localization geometry for case 1 is given in Fig. 2. The target's location is given by $[10\ 30]^{\mathrm{T}}$, while the sensor locations are given by $[0\ 0]^{\mathrm{T}}$, $[8\ -2]^{\mathrm{T}}$, $[12\ -5]^{\mathrm{T}}$, and $[20\ 1]^{\mathrm{T}}$, respectively. In Table I, we give the mean location estimate and RMS location error (RMSE) calculated over 10 000 simulation runs with a variance of $\sigma_d^2 = 0.004$.

From Table I, we note that the constrained optimization (GCLS) and the TML-GN algorithm perform almost identically (within numerical tolerances). Both numerical algorithms outperform the closed-form technique. In essence, this simulation demonstrates the performance of the three algorithms in a localization geometry that is reasonably suited to accurate localization. Hence, it is not surprising that both numerical localization techniques perform quite well. In the next simulation case, we will demonstrate the performance of the three algorithms in an adverse localization geometry.

In Fig. 3, we plot the RMSE over 10 000 simulation runs for a measurement error variance ranging from $\sigma_d^2 = 0.002$ to $\sigma_d^2 =$

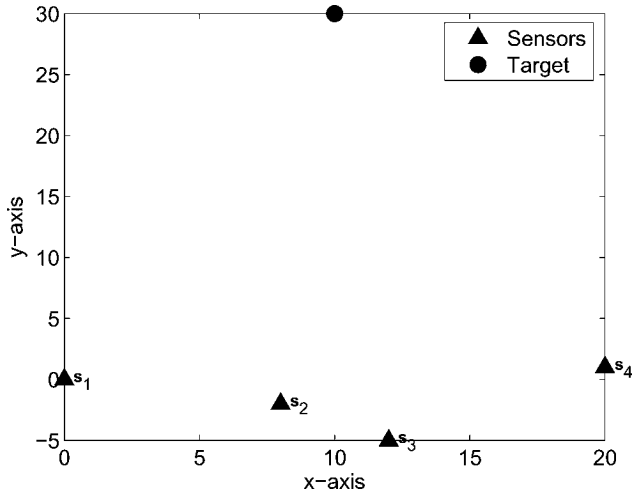

Fig. 2. Localization geometry for simulation case 1. In this case, the relative sensor–target geometry is well conditioned for accurate localization because the sensors and the target are not close to collinear.

TABLE I
LOCALIZATION PERFORMANCE FOR SIMULATION CASE 1

	Mean	RMSE
GCLS	$[10.00\ 30.02]^{\mathrm{T}}$	0.8837
TML-GN	$[9.99\ 30.02]^{\mathrm{T}}$	0.8959
Closed-Form (Remark 2)	$[10.15\ 30.09]^{\mathrm{T}}$	1.3705

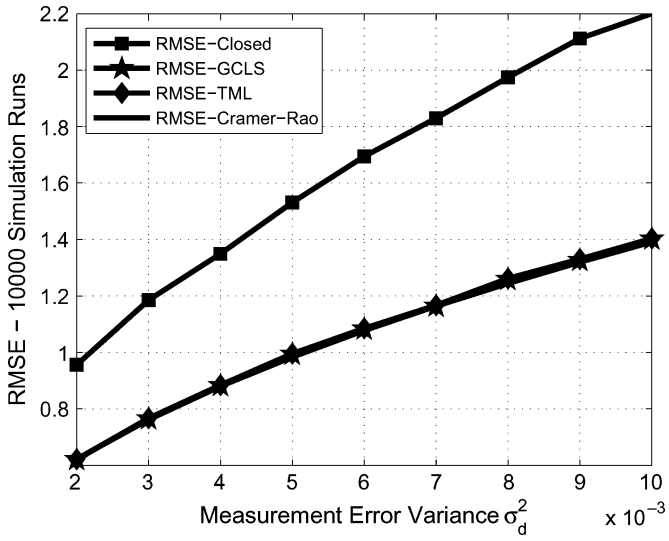

Fig. 3. RMSE performance for simulation case 1 with accurately known sensor locations. The performances of the TML-GN and GCLS algorithm are almost identical because both achieve a true ML estimate. Moreover, both achieve the Cramér–Rao lower bound as seen in the figure where all three RMSE curves essentially fall on top of each other.

0.01 and compare the closed form, TML-GN, GCLS, and the Cramér–Rao lower bound [37].

From Fig. 3, we can again note that in a reasonable localization geometry, both numerical ML techniques perform well and particularly in comparison to the Cramér–Rao bound.

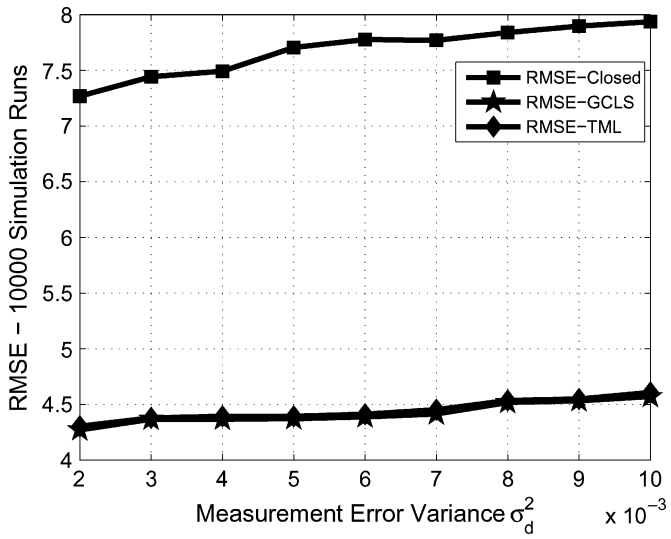

Fig. 4. RMSE performance for simulation case 1 with inaccurately known sensor locations. The performances of the TML-GN and GCLS algorithm are almost identical because both achieve a true ML estimate. Thus, the RMSE curves for both TML-GN and GCLS algorithms can be seen to fall on top of each other.

The Cramér–Rao bound was computed as in [8] and [37]. No "threshold" level of noise is observed within the considered noise range, above which performance of one or more algorithms collapses; the performances of TML-GN and GCLS are very close, and indeed close to the Cramér–Rao bound for *unbiased* estimators. Note that for a finite number of measurements (as we have here), both TML and our geometrically constrained formulation for ML estimation do *not* provide an unbiased estimate [32], [39], and so the similarity to the Cramér–Rao bound performance may not be significant [39]–[42].

The simulations considered thus far in this section are based on the assumption that each sensor's location is known accurately. In practice, this assumption is potentially unrealistic. We will thus simulate a localization scenario where the sensor locations are known inaccurately. Consider again the true sensor–target geometry illustrated in Fig. 2. The true range-difference values thus correspond to the range differences illustrated in this figure. However, the sensor locations used in the three different localization algorithms are erroneous. The erroneous sensor location values occur because the sensors themselves have not been completely/truthfully self-localized.

The erroneous sensor location values used by the sensors (and incorrectly assumed to be accurate) are Gaussian distributed about the true sensor locations with a standard deviation of 0.2 units. Each component (i.e., in both spatial dimensions) of each sensor location is independently corrupted by the relevant Gaussian error. In Fig. 3, we compare the closed form, TML-GN, and the GCLS algorithm by plotting the RMSE over 10 000 simulation runs for the described simulation scenario and for a measurement error variance ranging from $\sigma_d^2 = 0.002$ to $\sigma_d^2 = 0.01$.

Fig. 4 suggests that inaccurate sensor location values bias the target estimate of all the localization algorithms. The performance of the GCLS and TML-GN algorithms is significantly better than the closed-form linear algorithm. However, none of

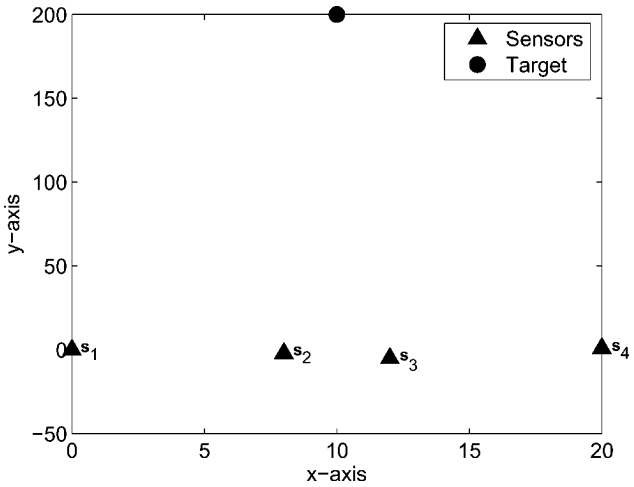

Fig. 5. Localization geometry for simulation case 2. In this case, the relative sensor–target geometry is adversely suited to accurate localization because the sensors and the target are far removed from each other.

the localization algorithms discussed in this paper are explicitly designed to deal with errors in the employed sensor location values. In particular, the GCLS and TML approaches are not true ML estimators in this case.

B. Simulation Case 2

The localization geometry for case 2 is given in Fig. 5. The target's location is now given by $[10\ 200]^{\mathrm{T}}$, while the four sensor's locations are as before and the measurement noise variance is $\sigma_d^2 = 0.004$. We have simply moved the target away from the sensors. The target's range to the sensor's baseline ratios is very large and we are essentially faced with a far-field localization problem. The particular location of the target and the long range mean that the target is likely to appear (in a noisy environment) almost collinear with the sensors. The relative sensor–target geometry is obviously adversely suited to accurate localization.

In this simulation case, we illustrate the advantage of our algorithm's localization-geometry-invariant initialization. This is by no means a trivial advantage. In Table II, we give the location estimate RMS error (RMSE) calculated over 10 000 simulation runs.[3]

From Table II, we note that the GCLS algorithm clearly outperforms the TML-GN algorithm, which diverged in approximately 1% of the simulation runs. While the closed-form technique cannot "diverge" in the sense defined, its performance is nevertheless unimpressive. The mean location estimate of the GCLS algorithm is quite good. For the simulation runs in which TML-GN diverges, the RMSE value for the GCLS estimate is 49.32.

[3]The TML-GN algorithm has diverged in a number of simulation runs leading to the large RMSE values depicted in Table II. We say an algorithm has diverged when the RMSE value exceeds 10^6. Note that this definition of divergence does not generally account for those location estimates that are merely of a very poor accuracy (particularly those found using the closed-form linear LS algorithms). For example, an estimate with an RMSE value of 10^5 is an example of a particularly poor solution. Rather, this definition of divergence specifically accounts for both numerical instability of the iterative techniques (which Gauss–Newton is known to exhibit) and divergence of iterative algorithms searching nonconvex surfaces. These algorithms can be affected by local stationary points or minima far removed from the vicinity of the true target location (or possibly minima on the infinite boundaries of the particular surface). In other words, we are trying to characterize those localization scenarios in which the TML algorithm will not generally (or easily) permit a globally optimal solution to found.

TABLE II
LOCALIZATION PERFORMANCE FOR SIMULATION CASE 2

	Mean	RMSE
GCLS	$[10.1\ 202.5]^{\mathrm{T}}$	46.56
All TML-GN Estimates[3]	$10^8 \times [0.74\ 1.28]^{\mathrm{T}}$	2.09×10^{10}
Non-Diverging TML-GN[4]	$[10.2\ 206.5]^{\mathrm{T}}$	61.32
Closed-Form (Remark 2)	$[10.4\ 245.4]^{\mathrm{T}}$	897.12

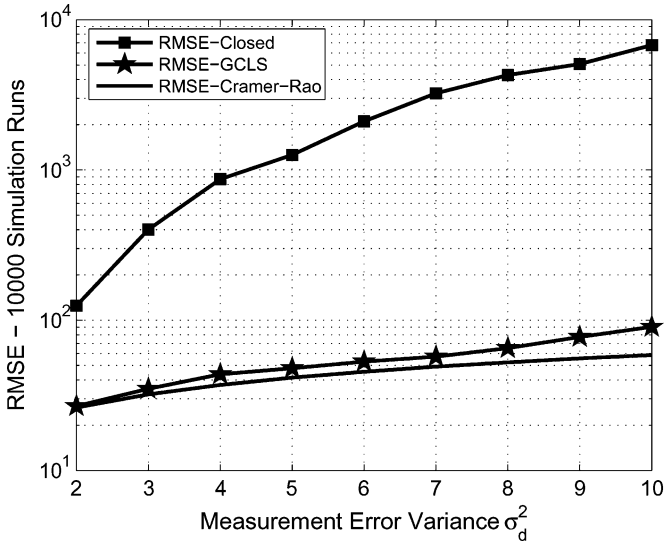

Fig. 6. RMSE performance for simulation case 2. The TML-GN algorithm diverges in an increasing number of simulation runs, e.g., see Table III, and is excluded from the graph.

TABLE III
DIVERGENCE OF THE TML-GN ALGORITHM IN SIMULATION CASE 2 AS A FUNCTION OF THE NOISE LEVEL

Variance σ_d^2	0.002	0.004	0.006	0.008	0.01
Approx. Divergence %	< 0.5	1	3	4	6

We believe the accuracy of GCLS stems from its numerical robustness and initialization invariance. In adverse localization geometries, it is not a trivial task to find an initial target location estimate that ensures that the TML algorithm will converge to the optimal solution.[4]

In Fig. 6, we plot the RMSE over 10 000 simulation runs for a measurement error variance ranging from $\sigma_d^2 = 0.002$ to $\sigma_d^2 = 0.01$ and compare the closed form, GCLS, and the Cramér–Rao lower bound for unbiased estimates. The TML-GN algorithm is omitted from the graph because it diverges in too many simulation runs (particularly when the variance is increased) as indicated in Table III. The RMSE axis is plotted on a log-scale in this case.

From Fig. 6, we note that even in an adverse localization geometry, our GCLS algorithm performs well when compared to

[4]Note that the difference between the RMSE values for the GCLS and the nondiverging TML-GN estimates (see Table II) could be a result of the employed divergence definition. In principle, if TML-GN converges to the globally optimal target solution, then the RMSE value should be the same as that for GCLS. Indeed, the median error values for GCLS and TML-GN are 24.6 and 25.4, respectively. Thus, the significance of this simulation result is that it shows GCLS can converge to the optimal target location estimate when TML-GN cannot.

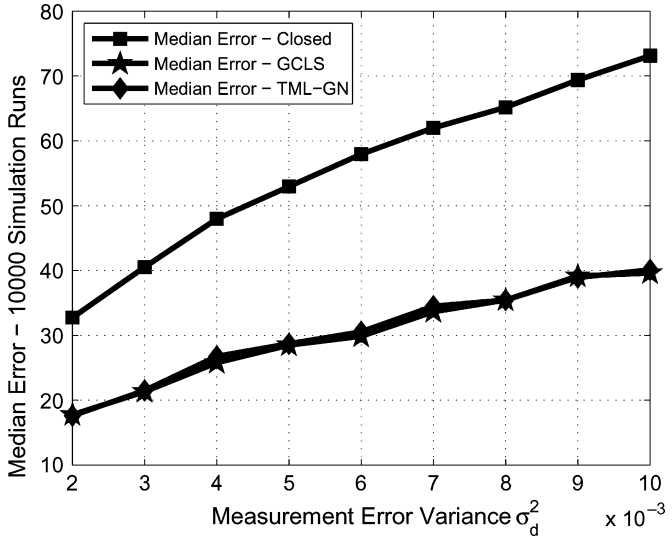

Fig. 7. Median error performance for simulation case 2. The median error curves for both TML-GN and GCLS algorithms fall almost on top of each other.

the Cramér–Rao bound. In Fig. 6, we notice the GCLS algorithm performance diverges away from the Cramér–Rao bound very slowly when compared with the linear LS algorithm. The adverse localization geometry contributes to this phenomenon, which was not observed in the first example. This divergence might be usable as a means for assessing (through simulation in specific geometries) under what measurement noise conditions an algorithm performs well (with respect to the Cramér–Rao bound). However, it is also unclear to us how meaningful a comparison can be of the performance of a biased estimate (GCLS) with an optimal unbiased estimate.

The TML-GN algorithm and the GCLS algorithm are seeking the same optimal (in the sense of ML) target position. However, their individual behavior is dependent on their respective formulations and on the iterative equations used to implement the algorithm. The TML-GN algorithm diverges in an increasing number of simulation runs with an increasing noise level as indicated in Table III. Under the assumed Gaussian error assumptions, the goal is to have the GCLS algorithm achieve an ML estimate while avoiding the divergence problems well known to plague the TML formulation. In Fig. 7, we plot the median location error over 10 000 simulation runs for a measurement error variance ranging from $\sigma_d^2 = 0.002$ to $\sigma_d^2 = 0.01$ and compare the closed form, GCLS, and the TML-GN algorithm.

The divergent TML-GN estimates have little effect on the median error value. However, in a number of simulation runs, the TML approach results in a difficult optimization problem that is prone to divergence as shown in Table III. Hence, the practical implementation of TML-GN is still unattractive and cannot be relied upon. Indeed, there is a general feeling in the literature that TML is unreliable in practice. Essentially, the GCLS algorithm inherits the positive aspects of the TML algorithm, e.g., see Fig. 7, while avoiding the negative aspects, e.g., see Table III.

Remark 5: Why should systematic localization with GCLS work better than that for TML-GN? While an argument with all the rigor of a theorem is hard to construct, at least a heuristic argument can be given. The initialization of the GCLS algorithm necessarily gives an initial error in the estimate of the measurement noise values, which is upper bounded by approximately four or five times the standard deviation of each error. On the other hand, the initial error in the position estimate for TML-GN is geometrically dependent; if, for example, the closed-form estimate is used to initialize the TML-GN iteration, the error could be very large, depending on the condition number of the matrix $\widehat{\mathbf{A}}$; see Remark 2.

TABLE IV
AVERAGE MATRIX CONDITION NUMBER OF $\widehat{\mathbf{A}}$; SEE REMARK 2, AS A FUNCTION OF THE NOISE LEVEL

Variance σ_d^2	0.002	0.004	0.006	0.008	0.01
Mean Cond. No.	306.31	373.23	503.36	720.22	870.92

In fact, Table IV compares the averaged (over 10 000 simulation runs) condition number of $\widehat{\mathbf{A}}$. A comparison of Table IV with Table III shows that this condition number is a good measure of the propensity or otherwise of the TML-GN algorithm to converge.

Of course, the condition number is actually affected by a number of factors each of which contributes to the propensity of TML-GN to diverge. These factors include not only the relative sensor–target geometry but also the measurement noise levels (albeit to a lesser degree). Actually, the measurement noise level is itself a significant factor in the propensity of TML-GN convergence as indicated in Table III, quite apart from its effect on the conditioning of $\widehat{\mathbf{A}}$ as indicated in Table IV.

C. Simulation Case 3

The target's location is given by $[50\ 200]^{\mathrm{T}}$ and the locations of $n \in \{10, 50, 100\}$ sensors are randomly distributed according to a uniform distribution such that their position components are bounded according to $x \in [0, 100]$ and $y \in [0, 25]$. The localization geometry in this case is random. Thus, in some simulation runs, the geometry is likely to be adversely suited to accurate localization, while in other simulation runs, the geometry might be well suited (or reasonably suited) to accurate localization. Despite the sensor positions being random, we use the best initialization possible, which is independent of the geometry for GCLS and uses the closed-form solution (and thus is geometry dependent) for TML-GN.

In this simulation example, we compare the RMS position errors of GCLS, TML-GN, and the closed-form technique discussed in Remark 2. The measurement noise variance is $\sigma_d^2 = 0.004$. The number of sensors $n \in \{10, 50, 100\}$ is increased to illustrate the relative performance of the given localization algorithms in situations involving greater than average numbers of sensors. We also compare the computational expense of our geometrically constrained approach to the Gauss–Newton-based TML approach by finding the mean and median number of iterations required to reach a solution. In Table V, we give the location estimate RMSE calculated over 10 000 simulation runs.

From Table V, we note that the RMSE performance of the GCLS algorithm and the TML-GN algorithm are almost identical on average for this example case when the number of sensors is increased (e.g., above 50). Actually, the difference in the closed-form algorithm's performance also becomes negligible

TABLE V
LOCALIZATION PERFORMANCE FOR SIMULATION CASE 3

	GCLS	TML-GN	Closed (see Remark 2)
RMSE - 10 Sensors	1.9503	2.1127	2.7381
RMSE - 50 Sensors	0.4569	0.4598	0.4725
RMSE - 100 Sensors	0.2011	0.2134	0.2161

TABLE VI
COMPUTATIONAL BURDEN IN TERMS OF THE NUMBER OF ITERATIONS FOR SIMULATION CASE 3

No. Sensors	Mean GCLS	Mean TML-GN	Median GCLS	Median TML-GN
10	8.3800	2.2550	8	2
50	19.8560	2.4850	17	2
100	52.5353	2.5740	50	3

as the number of sensors increases. Indeed, the localization geometry is generally reasonable and thus one would expect most algorithms to perform well. In Table VI, we give the mean and median number of iterations required to reach a solution analyzed over 10 000 simulation runs.

From Table VI, we note that our technique is more computationally expensive than the TML approach using Gauss–Newton. Indeed, the computational expense of the GCLS algorithm grows with the number of sensors because there exists one additional constraint with the addition of each sensor (> 4 in $\mathbb{R}^2$). This additional burden is not particularly present in the Gauss–Newton-based TML algorithm. An interesting point that is particularly relevant is that as the number of sensors increases, the accuracy (measured via the RMSE value) of the closed-form technique (discussed in Remark 2) increases. Moreover, the closed-form technique can be implemented quite efficiently with modern linear algebra software.

D. General Discussion

From the simulations in $\mathbb{R}^2$, we note that the constrained optimization estimate outperforms the other approaches illustrated in particular in adverse localization geometries. Similar results can be demonstrated for localization systems in $\mathbb{R}^3$.

The TML approach unfortunately suffers from initialization problems and, in general, is not practically suited to localization in such geometries, albeit the underlying goal of TML is to find an optimal location solution. Note the convergence of TML is (in part) dependent on the accuracy of the chosen closed-form method used to initialize TML. Our GCLS algorithm addresses the practical problems inherent in the TML algorithm by removing the effect of the geometry on the initialization routines. That is, our GCLS algorithm initialization is geometry invariant and only depends on the expected values of the measurement errors.

Finally, we remarked previously that although we employ an LS objective function, we are by no means restricted to doing so. The geometric constraint is invariant to the cost function associated with the optimization problem and if it turns out that some other objective is better suited to a given problem then it is straightforward to adapt our approach appropriately. Note that in this case, the GCLS algorithm would bear no relationship to the TML formulated algorithm.

VI. DIRECTIONS FOR FUTURE WORK

In this section, we discuss some directions for possible future work. First, the proposed algorithm assumes that the sensor locations are known accurately. Hence, it would be practically beneficial to extend the proposed optimal localization algorithm to explicitly account for errors in these (assumed known) sensor location values. Similarly, nonconstant signal propagation speeds could arise in practice, for which the proposed algorithm would yield suboptimal target location estimates. Integrating consideration of such issues into the proposed algorithm is not trivial and illustrates an interesting direction for future work.

The concept of robust localization using geometric constraints is a possible future research direction for which the proposed geometric-constraint-based estimation algorithm is highly suited. That is, it would be helpful to evaluate the performance of different cost functions, i.e., other than the LS cost functions. In this way, robust localization algorithms can be designed to account for unknown or partially known error statistics and different error distribution models. For example, the ℓ^1-norm is generally considered to be robust against measurement error outliers and is a possible candidate for experimentation.

The relative target–sensor geometry has been rigorously examined for time-of-arrival-based localization in [37]. When considering a *remote* target where the target's range-to-sensor-baseline ratio is large, then it is likely that the target will appear approximately collinear with the sensors in the sense that the angle subtended at the target by the two lines joining any two sensors to the target will be very small. The problem of determining an appropriate localization algorithm to employ in a particular scenario is thus a practically significant research question. For example, the closed-form linear LS algorithm may perform well when the number of sensors is large and/or the localization geometry is not adverse to good localization accuracy. However, they are not statistically optimal. Thus, a characterization of the conditions under which a particular algorithm should (or can) perform well would be a significant result.

Another interesting question flows from the fact that algorithms may converge to highly inaccurate solutions. If we assume that our numerical algorithm has converged to a solution, then it would be desirable for one to ascertain whether this solution is in a neighborhood enclosing the correct point. Is it possible to characterize the region of attraction based purely on the geometry of the target and the sensors? Moreover, are there any external or inherent characteristics of the problem that permit one to draw such a conclusion?

VII. CONCLUDING REMARKS

This paper has introduced a constraint on the passive range-difference measurement errors. The constraint we have derived accounts for the underlying geometry, the measurements, and the nature of the true measurement errors. The constraint allows us to estimate the errors such that the system is consistent

with the geometrical requirements. The problem is formulated as a constrained optimization problem and the resulting location estimate is compared with the traditional LS (ML) approach. We illustrated that our technique is particularly suited to adverse localization geometries. The constraint is independent of the chosen cost function and the optimization algorithm may be initialized independently of the localization geometry. The comparison shows that from the point of view of guaranteeing localization accuracy, especially in adverse localization geometries, our proposed method is the superior choice for TDOA-based (or RDOA-based) localization especially as compared to TML and the simple closed-form pseudo-LS algorithms.

APPENDIX
A FICTITIOUS POSITION ESTIMATE FOR THE GCLS ALGORITHM

Consider the GCLS algorithm (applied in $\mathbb{R}^q, q \in \{2,3\}$) described in Sections III and IV. Let us denote the true target position as $\mathbf{p}$ and let $\mathbf{d} = [d_{12}, \ldots, d_{1n}]^{\mathrm{T}}$ and $\widehat{\mathbf{d}} = [\widehat{d}_{12}, \ldots, \widehat{d}_{1n}]^{\mathrm{T}}$, where n is the number of sensors and the actual and measured range-difference terms $d_{1i}, \widehat{d}_{1i} = d_{1i} - e_{1i}, \forall i \in \{2, \ldots, n\}$ are as defined in Section III. We assume without loss of generality that sensor 1 is located at the coordinate origin.

As stated in Sections III and IV, the GCLS algorithm employs iterations of the form

$$\mathbf{e}_{k+1} = \mathbf{e}_k + \boldsymbol{\delta}_{\mathbf{e}k}$$

where $\mathbf{e}_k$ is the estimate of $\mathbf{e} = \mathbf{d} - \widehat{\mathbf{d}}$ obtained at the k^{th} iteration step. Defining the fictitious estimate $\mathbf{d}_k$ of $\mathbf{d}$ as

$$\mathbf{d}_k \triangleq \mathbf{e}_k + \widehat{\mathbf{d}}$$

it follows that

$$\mathbf{d}_{k+1} = \mathbf{d}_k + \boldsymbol{\delta}_{\mathbf{e}k}.$$

As discussed in Remark 2, we can define a closed-form geometrical mapping $\mathcal{M}_1$ that maps a vector $\widetilde{\mathbf{d}} \in \mathbb{R}^{n-1}$ of range-difference estimates (an estimate of $\mathbf{d}$) to a target position estimate $\widetilde{\mathbf{p}} \in \mathbb{R}^d$ (an estimate of $\mathbf{p}$). Defining the fictitious estimate $\widetilde{\mathbf{p}}_k$ of $\mathbf{p}$ at the kth iteration step as

$$\widetilde{\boldsymbol{p}}_k \triangleq \mathcal{M}_1(\mathbf{d}_k)$$

the step change in the fictitious estimate term satisfies

$$\boldsymbol{\delta}_{\widetilde{\boldsymbol{p}}_k} \triangleq \widetilde{\boldsymbol{p}}_{k+1} - \widetilde{\boldsymbol{p}}_k = \mathcal{M}_1(\mathbf{d}_{k+1}) - \mathcal{M}_1(\mathbf{d}_k).$$

Therefore, assuming that $\mathcal{M}_1$ is Lipschitz in the (compact) domain of interest $\mathcal{C} \subset \mathbb{R}^{n-1}$ with a certain Lipschitz coefficient k_l, i.e.,

$$\left\|\mathcal{M}_1(\bar{\mathbf{d}}_1) - \mathcal{M}_1(\bar{\mathbf{d}}_2)\right\| \leq k_l \|\bar{\mathbf{d}}_1 - \bar{\mathbf{d}}_2\|, \ \forall \mathbf{d}_1, \mathbf{d}_2 \in \mathcal{C}$$

we have

$$\|\boldsymbol{\delta}_{\widetilde{\boldsymbol{p}}_k}\| \leq k_l \|\boldsymbol{\delta}_{\mathbf{e}k}\|.$$

The last inequality implies that once $\delta_{\mathbf{e}k}$ is below a certain threshold $\bar{\delta} > 0$, $\delta_{\widetilde{\mathbf{p}}_k}$ is bounded by $k_l \bar{\delta}$.

It can be observed from the equations in Section III leading to Remark 2 that the above Lipschitz assumption is a mild one, unless the sensor distribution geometry is ill conditioned (e.g., all the sensors are collinear). Furthermore, a nominal value for k_l may be predefined based on the known sensor distribution geometry and *a priori* information about the target position.

REFERENCES

[1] S. C. Nardone, A. G. Lindgren, and K. F. Gong, "Fundamental properties and performance of conventional bearings-only target motion analysis," *IEEE Trans. Autom. Control*, vol. AC-29, no. 9, pp. 775–787, Sep. 1984.

[2] M. Gavish and A. J. Weiss, "Performance analysis of bearing-only target location algorithms," *IEEE Trans. Aerosp. Electron. Syst.*, vol. 28, no. 3, pp. 817–827, Jul. 1992.

[3] N. Patwari, A. O. Hero, M. Perkins, N. S. Correal, and R. J. O'Dea, "Relative location estimation in wireless sensor networks," *IEEE Trans. Signal Process.*, vol. 51, no. 8, pp. 2137–2148, Aug. 2003.

[4] "Special issue on time-delay estimation," *IEEE Trans. Acoust. Speech Signal Process.*, vol. ASSP-29, no. 3, pp. 461–623, Jun. 1981.

[5] B. Friedlander, "A passive localization algorithm and its accuracy analysis," *IEEE J. Ocean. Eng.*, vol. 12, no. 1, pp. 234–245, Jan. 1987.

[6] J. O. Smith and J. S. Abel, "The spherical interpolation method of source localization," *IEEE J. Ocean. Eng.*, vol. 12, no. 1, pp. 246–252, Jan. 1987.

[7] G. C. Carter and E. R. Robinson, "Ocean effects on time delay estimation requiring adaptation," *IEEE J. Ocean. Eng.*, vol. 18, no. 4, pp. 367–378, Oct. 1993.

[8] Y. T. Chan and K. C. Ho, "A simple and efficient estimator for hyperbolic location," *IEEE Trans. Signal Process.*, vol. 42, no. 8, pp. 1905–1915, Aug. 1994.

[9] Y. Huang, J. Benesty, G. W. Elko, and R. M. Mersereau, "Real-time passive source localization: A practical linear-correction least-squares approach," *IEEE Trans. Speech Audio Process.*, vol. 9, no. 8, pp. 943–956, Nov. 2001.

[10] J. C. Hassab, *Underwater Signal and Data Processing*. Boca Raton, FL: CRC Press, 1989.

[11] J. H. Collins and P. M. Grant, "A review of current and future components for electronic warfare receivers," *IEEE Trans. Sonics Ultrason.*, vol. 28, no. 3, pp. 117–125, May 1981.

[12] A. E. Spezio, "Electronic warfare systems," *IEEE Trans. Microw. Theory Tech.*, vol. 50, no. 3, pp. 633–644, Mar. 2002.

[13] I. A. Getting, "The global positioning system," *IEEE Spectrum*, vol. 30, no. 12, pp. 36–38, Dec. 1993, 43–47.

[14] W. H. Foy, "Position-location solutions by Taylor-series estimation," *IEEE Trans. Aerosp. Electron. Syst.*, vol. AES-12, no. 2, pp. 187–194, Mar. 1976.

[15] M. Wax and T. Kailath, "Optimum localization of multiple sources by passive arrays," *IEEE Trans. Acoust. Speech Signal Process.*, vol. ASSP-31, no. 5, pp. 608–614, May 1983.

[16] K. Dogancay, "Emitter localization using clustering-based bearing association," *IEEE Trans. Aerosp. Electron. Syst.*, vol. 41, no. 2, pp. 525–536, Apr. 2005.

[17] R. Schmidt, "A new approach to geometry of range difference location," *IEEE Trans. Aerosp. Electron. Syst.*, vol. 8, no. AES-6, pp. 821–835, Nov. 1972.

[18] J. O. Smith and J. S. Abel, "Closed-form least-squares source location estimation from range-difference measurements," *IEEE Trans. Acoust. Speech Signal Process.*, vol. ASSP-35, no. 12, pp. 1661–1669, Dec. 1987.

[19] H. C. Schau and A. Z. Robinson, "Passive source localization employing intersecting spherical surfaces from time-of-arrival differences," *IEEE Trans. Acoust. Speech Signal Process.*, vol. ASSP-35, no. 8, pp. 1223–1225, Aug. 1987.

[20] D. J. Torrieri, "Statistical theory of passive location systems," *IEEE Trans. Aerosp. Electron. Syst.*, vol. AES-20, no. 2, pp. 183–198, Mar. 1984.

[21] R. I. Hartley and P. Sturm, "Triangulation," *Comput. Vis. Image Understanding*, vol. 68, no. 2, pp. 146–157, Nov. 1997.

[22] M. Cao, B. D. O. Anderson, and A. S. Morse, "Sensor network localization with imprecise distances," *Syst. Control Lett.*, vol. 55, no. 11, pp. 887–893, Nov. 2006.

[23] A. N. Bishop, B. D. O. Anderson, B. Fidan, P. N. Pathirana, and G. Mao, "Bearing-only localization using geometrically constrained optimization," *IEEE Trans. Aerosp. Electron. Syst.*, to be published.

[24] A. N. Bishop, B. Fidan, K. Dogancay, B. D. O. Anderson, and P. N. Pathirana, "Exploiting geometry for improved hybrid AOA/TDOA-based localization," *Signal Process.*, vol. 88, no. 7, pp. 1775–1791, July 2008.

[25] M. S. Brandstein, J. E. Adcock, and H. F. Silverman, "A closed-form location estimator for use with room environment microphone arrays," *IEEE Trans. Speech Audio Process.*, vol. 5, no. 1, pp. 45–50, Jan. 1997.

[26] R. Fletcher, *Practical Methods of Optimization*. New York: Wiley, 1981.
[27] D. P. Bertsekas, *Constrained Optimization and Lagrange Multiplier Methods*. Belmont, MA: Athena Scientific, 1996.
[28] P. E. Gill, W. Murray, and M. H. Wright, *Practical Optimization*. London, U.K.: Academic, 1981.
[29] S. K. Agrawal and B. C. Fabien, *Optimization of Dynamic Systems*. Boston, MA: Kluwer, 1999.
[30] P. Wolfe, "Convergence conditions for ascent methods," *SIAM Rev.*, vol. 11, no. 2, pp. 226–235, Apr. 1969.
[31] P. Wolfe, "Convergence conditions for ascent methods. II: Some corrections," *SIAM Rev.*, vol. 13, no. 2, pp. 185–188, Apr. 1971.
[32] H. L. Van Trees, *Detection, Estimation and Modulation Theory*. New York: Wiley, 1968.
[33] M. S. Brandstein, J. E. Adcock, and H. F. Silverman, "Microphone-array localization error estimation with application to sensor placement," *J. Acoust. Soc. Amer.*, vol. 99, no. 6, pp. 3807–3816, Jun. 1996.
[34] J. R. Rice and J. S. White, "Norms for smoothing and estimation," *SIAM Rev.*, vol. 6, no. 3, pp. 243–256, Jul. 1964.
[35] J. F. Arnold, Y. Bar-Shalom, R. Estrada, and R. A. Mucci, "Target parameter estimation using measurements acquired with a small number of sensors," *IEEE J. Ocean. Eng.*, vol. 8, no. 3, pp. 163–172, Jul. 1983.
[36] A. N. Bishop, B. Fidan, B. D. O. Anderson, K. Dogancay, and P. N. Pathirana, "Optimality analysis of sensor-target geometries in passive localization: Part 1—Bearing-only localization," in *Proc. 3rd Int. Conf.n Intell. Sens. Sens. Netw. Inf. Process.*, Melbourne, Australia, Dec. 2007, pp. 7–12.
[37] A. N. Bishop, B. Fidan, B. D. O. Anderson, P. N. Pathirana, and K. Dogancay, "Optimality analysis of sensor-target geometries in passive localization: Part 2—Time-of-arrival based localization," in *Proc. 3rd Int. Conf. Intell. Sens. Sens. Netw. Inf. Process.*, Melbourne, Australia, Dec. 2007, pp. 13–18.
[38] K. Dogancay and H. Hmam, "Optimal angular sensor separation for AOA localization," *Signal Process.*, vol. 88, no. 5, pp. 1248–1260, May 2008.
[39] Y. C. Eldar, "Minimum variance in biased estimation: Bounds and asymptotically optimal estimators," *IEEE Trans. Signal Process.*, vol. 52, no. 7, pp. 1915–1930, Jul. 2004.
[40] A. O. Hero, J. A. Fessler, and U. Usman, "Exploring estimator bias-variance tradeoffs using the uniform CR bound," *IEEE Trans. Signal Process.*, vol. 44, no. 8, pp. 2026–2041, Aug. 1996.
[41] P. Stoica and T. L. Marzetta, "Parameter estimation problems with singular information matrices," *IEEE Trans. Signal Process.*, vol. 49, no. 1, pp. 87–90, Jan. 2001.
[42] Y. C. Eldar, "Uniformly improving the Cramer-Rao bound and maximum-likelihood estimation," *IEEE Trans. Signal Process.*, vol. 54, no. 8, pp. 2943–2956, Aug. 2006.

Adrian N. Bishop, photograph and biography not available at the time of publication.

Barış Fidan (S'02–M'03) received the B.S. degrees in electrical engineering and mathematics from Middle East Technical University, Ankara, Turkey, in 1996, the M.S. degree in electrical engineering from Bilkent University, Ankara, Turkey, in 1998, and the Ph.D. degree in electrical engineering from the University of Southern California, Los Angeles, in 2003.

He has been with National ICT Australia, Canberra, A.C.T., Australia, and the Research School of Information Sciences and Engineering, Australian National University, Canberra, A.C.T., Australia since 2005, where he is currently a Senior Researcher. His research interests include autonomous formations, sensor networks, cooperative localization, adaptive and nonlinear control, switching and hybrid systems, mechatronics, and various control applications.

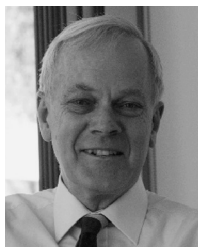

Brian D. O. Anderson (S'62–M'66–SM'74–F'75–LF'06) was born in Sydney, Australia, and received his undergraduate education at the University of Sydney, Sydney, Australia, with majors in pure mathematics and electrical engineering. He received the Ph.D. degree in electrical engineering from Stanford University, Stanford, CA, in 1966.

He worked in industry in Silicon Valley and served as a Faculty Member in the Department of Electrical Engineering, Stanford University. He was Professor of Electrical Engineering at the University of Newcastle, Australia, from 1967 to 1981 and is now a Distinguished Professor at the Australian National University, Canberra, A.C.T., Australia and a Distinguished Researcher at the National ICT Australia, Canberra, A.C.T., Australia. His interests are in control and signal processing.

Dr. Anderson is a Fellow of Royal Society London, Australian Academy of Science, Australian Academy of Technological Sciences and Engineering, Honorary Fellow of the Institution of Engineers, Australia, and Foreign Associate of the U.S. National Academy of Engineering. He holds doctorates (*honoris causa*) from the Université Catholique de Louvain, Belgium, Swiss Federal Institute of Technology, Zürich, Switzerland, Universities of Sydney, Melbourne, New South Wales, and Newcastle. He served a term as President of the International Federation of Automatic Control from 1990 to 1993 and as President of the Australian Academy of Science between 1998 and 2002. His awards include the IEEE Control Systems Award of 1997, the 2001 IEEE James H. Mulligan, Jr. Education Medal, and the Guillemin-Cauer Award, IEEE Circuits and Systems Society in 1992 and 2001, the Bode Prize of the IEEE Control System Society in 1992, and the Senior Prize of the IEEE TRANSACTIONS ON ACOUSTICS, SPEECH AND SIGNAL PROCESSING in 1986.

Kutluyıl Doğançay (S'90–M'91–SM'01) received the B.S. degree with honors in electrical and electronic engineering from Boğaziçi University, Istanbul, Turkey, in 1989, the M.Sc. degree in communications and signal processing from the University of London, London, U.K., in 1992, and the Ph.D. degree in telecommunications engineering from The Australian National University, Canberra, A.C.T., Australia, in 1996.

Since November 1999, he has been with the School of Electrical and Information Engineering, University of South Australia, where he is currently an Associate Professor. His research interests span statistical and adaptive signal processing, and its application to defence and communication systems. He serves as a consultant to defence and private industry in signal processing and communications related projects.

Dr. Doğançay has been on the technical program committee of several international conferences including EUSIPCO 2008. He was the Signal Processing and Communications Program Chair of the 2007 Information, Decision and Control Conference. He is an Editor for the *Signal Processing* journal of EURASIP. He received the 2005–2006 Tall Poppy Science Award of the Australian Institute of Political Science. He is currently serving as Chair of the IEEE South Australia Communications and Signal Processing Chapter.

Pubudu N. Pathirana (M'08–SM'08) was born in 1970 in Matara, Sri Lanka, and was educated in Royal College Colombo. He received the B.E. degree (first class honors) in electrical engineering and the B.Sc. degree in mathematics in 1996, and the Ph.D. degree in electrical engineering in 2000 from the University of Western Australia sponsored by the government of Australia on EMSS and IPRS scholarships, respectively.

In 1997–1998, he worked as a Research Engineer in the industry in Singapore and in Sri Lanka. He was a Postdoctoral Research Fellow at Oxford University, Oxford, U.K., 2001 on a Ford Motor Co. (USA) project, a Research Fellow at the School of Electrical Engineering and Telecommunications, University of New South Wales, Sydney, Australia, and a Consultant to the Defence Science and Technology Organization (DSTO), Australia, in 2002. Currently, he is with the School of Engineering and Technology, Deakin University, Geelong, Australia, and his current research interests include missile guidance, autonomous systems, computer integrated manufacturing, vision-based navigation systems, quality-of-service (QoS) management, and mobile/wireless networks.